Refractive scattering evidence from multifrequency scintillation spectra observed at auroral latitudes

B. Forte[1]

[1] During October 2003 major geomagnetic storm, intensity scintillations on radio signals at 150 MHz and 400 MHz transmitted coherently from Tsykada beacon satellites have been observed. Through the analysis of intensity fluctuation spectra, evidence of refractive scattering from large scale ionospheric irregularities in the spatial plasma density distribution is found. The events can indeed be explained by using the refractive scattering theory developed by Booker and MajidiAhi (1981). The presence of refractive scattering is particularly evident in strong scintillation events, where spectral saturation may well occur. The observed intensity spectra fit the shape of theoretical predictions of the refractive theory. This provides useful insights about spectral slope, Fresnel scale, and the scale of irregularities producing the observed intensity scintillations actually present in the ionosphere.

Citation: Forte, B. (2008), Refractive scattering evidence from multifrequency scintillation spectra observed at auroral latitudes, *Radio Sci.*, *43*, RS2012, doi:10.1029/2007RS003715.

1. Introduction

[2] Electromagnetic waves propagating through an irregular medium may be scattered by refractive index fluctuations. When small angle scattering occurs, intensity and phase fluctuations may be observed on the propagating waves.

[3] Usually, two mechanisms may be responsible for the scintillation of radio waves: weak scattering (occurring for low scintillation levels) and strong scattering (occurring for high scintillation levels) [*Rino*, 1979a, 1979b]. The problem is often modelled by means of a thin phase changing screen which allows both weak and strong scattering to be easily described. Nevertheless, attention should be paid on this simplified approach, as the thin phase screen implies a process based on strong single scattering rather than on weak multiple scattering, also leading to high scintillation levels. The thin phase screen approach suggests a diffractive scattering of the traversing electromagnetic wave, for both weak and strong cases. Diffractive scattering is due to refractive index irregulaties with scales smaller than the Fresnel scale corresponding to the link geometry. In the case of transionospheric radio signals, diffractive scattering usu-ally dominates when the ionisation density fluctuations are relatively low. On the contrary, when they are high, refractive scattering appears to be the dominant mechanism. Refractive scattering is produced by plasma density irregularities with scales larger than the Fresnel scale. When refractive scattering dominates, besides the usual Fresnel scale associated with the propagation problem, other scales (such as the peak scale, the focal scale, and the lens scale) for plasma density structures come into play [*Booker and MajidiAhi*, 1981].

[4] The concept of refractive scattering may help in explaining strong scintillation events observed on VHF beacon radio signals transmitted from Tsykada polar low Earth orbiting (LEO) satellites, at European auroral ground stations during the intense geomagnetic storm occurred at the end of October 2003. These events were characterised by fluctuations in the ionisation density distribution [*Mitchell et al.*, 2005; *Foster and Rideout*, 2005] far beyond the limit below which a diffractive mechanism could well explain the observations. Here, use is made of the theory developed by *Booker and MajidiAhi* [1981] for explaining strong scintillation events at auroral latitudes. Similar analyses have already been done for low latitude scintillation events [*Vats et al.*, 1981; *Crain et al.*, 1979].

2. Experimental Data

[5] Radio signals coherently transmitted from Tsykada polar LEO beacon satellites at 150 MHz and 400 MHz

---

[1]Centre for Atmospheric Research, University of Nova Gorica, Nova Gorica, Slovenia.

Figure 1. The ground stations used for recording Tsykada signals: Tromso (TRO), Kiruna (KIR), Lulea (LUL), and Kokkola (KOK).

have been received at some ground stations, nearly aligned for ionospheric tomography purposes (Figure 1). Both signal intensity and phase are sampled at a 50 Hz rate, detrended in order to distinguish ionospheric scintillations from other spectral components, and used for calculating both the intensity scintillation index S_4 [*Briggs and Parkin*, 1963] and the classical phase scintillation index σ_ϕ. Here, misleading detrending effects at high latitudes are neglected, as the main interest is in intensity fluctuations only [*Forte and Radicella*, 2002]. A rough estimate of phase scintillation is here limited to the classical phase scintillation index σ_ϕ, which is not an appropriate parameter for estimating the phase scintillation activity, particularly at high latitudes [*Forte*, 2005].

[6] By assuming ergodic quantities, the ensemble averages involved in the S_4 calculation are replaced by the time averages over a 20 sec period. The problem geometry, coupled with pierce point relative drift at ionospheric altitudes, justifies such an assumption, as it was also recognised in the similar Wideband experiment geometry [*Fremouw et al.*, 1978].

[7] Let a plane wave be normally incident on a generic phase changing screen. If the intensity spectrum in a reception plane at a distance z beyond the screen is $I(k)$, the square of the scintillation index is given by [*Tatarskii*, 1967]:

$$S_4^2 = \frac{1}{2\pi} \int_0^\infty I(k)dk \qquad (1)$$

where k is the spatial frequency and $I(k)$ is the contribution to S_4^2 per unit spatial frequency. On the other hand

$$S_4^2 = \int_0^\infty S_4^2(k)dk \qquad (2)$$

so that

$$S_4^2(k) = \frac{I(k)}{2\pi} \qquad (3)$$

Let $\Phi_I^{ex}(k)$ be the experimental power spectral density for intensity fluctuations, so that

$$\sigma_I^2 = \frac{1}{2\pi} \int_0^\infty \Phi_I^{ex}(k)dk \qquad (4)$$

Since

$$S_4^2 = \frac{\sigma_I^2}{\overline{I}^2} \qquad (5)$$

it follows

$$S_4^2(k) = \frac{\Phi_I^{ex}(k)}{\overline{I}^2} \qquad (6)$$

where $\overline{I}$ denotes an ensemble average. Both experimental and theoretical results are presented in terms of $S_4^2(k)$ rather than in terms of $\Phi_I^{ex}(k)$.

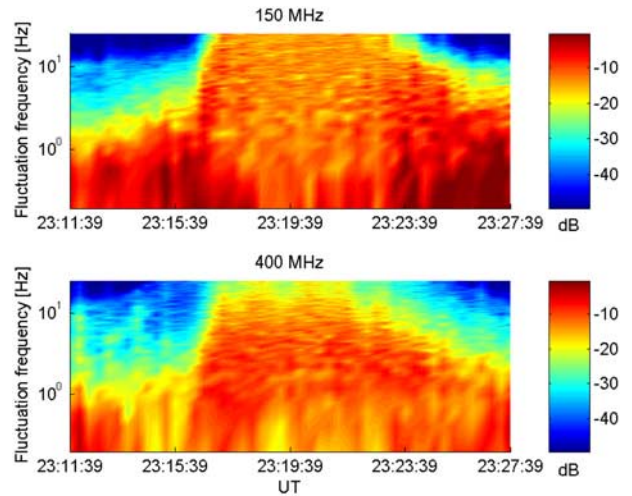[8] Figure 2 shows intensity spectra observed simultaneously on the two signals (150 MHz and 400 MHz) at

Figure 2. Overview of the intensity spectra observed at 150 MHz and 400 MHz at the ground station located in Kiruna during the night of 30 October 2003, for a satellite pass starting at 23:11:39 UT.
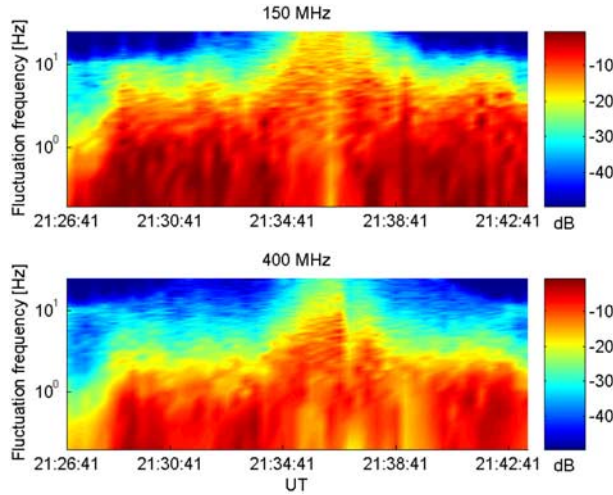
Figure 3. Overview of the intensity spectra observed at 150 MHz and 400 MHz at the ground station located in Lulea during the night of 30 October 2003, for a satellite pass starting at 21:26:41 UT.

the ground station located in Kiruna, during the night of 30 October 2003, in the middle of a main geomagnetic storm phase. These intensity spectra refer to the satellite pass beginning at 23:11:39 UT over Kiruna (Lat.: 67.84°N, Lon.: 20.41°E, L = 5.6). Figure 3 shows a similar overview of intensity spectra observed at Lulea (Lat.: 65.58°N, Lon.: 22.17°E, L = 4.7) during the night of 30 October 2003, for a satellite pass beginning at 21:26:41 UT, while Figure 4 shows the situation recorded at Kokkola (Lat.: 63.83°N, Lon.: 23.06°E, L = 4.2) during the same night for a satellite pass beginning at 19:28:59 UT.

[9] Figure 5 shows the intensity scintillation indices for the 150 MHz signal (dotted line) and the 400 MHz signal (dashed line) referring to the intensity spectra depicted in Figures 2, 3, and 4.

[10] It may be observed that intensity spectra modify their shape, broadening towards smaller spatial scales (i.e., higher fluctuation frequencies), as the scintillation activity increases to saturating conditions. This feature seems to be common to all observing sites and times, suggesting a situation similar to that already observed in the past at equatorial latitudes with VHF/UHF signals [*Vats et al.*, 1981] and with SHF signals [*Crain et al.*, 1979], where the rms fluctuation of phase was found in excess of one radian making the weak scattering theory not suitable for the explanation of the events observed. Those events were indeed explained in terms of refractive scattering by large scale ionisation irregularities,

which seem consistent with the occurrence of equatorial plumes [*Vats et al.*, 1981].

3. Theoretical Intensity Spectra According to Refractive Scattering Theory

[11] Let the ionospheric F region be modelled as a layer with a mean ionisation density N and a uniform mean square fractional fluctuation of ionisation density $\overline{\left(\frac{\Delta N}{N}\right)^2}$. If the transionospheric electromagnetic radiation is coming from a point source at a zenith angle χ on the ground, the mean square fluctuation of phase due to the propagation through the F region may be assumed as

$$\overline{(\Delta\phi)^2} = 4r_e^2 N^2 \overline{\left(\frac{\Delta N}{N}\right)^2} \lambda^2 L_0 D \sec\chi \qquad (7)$$

where r_e is the classical electron radius, L_0 is the outer scale, D is the layer thickness, and λ is the wavelength of the radiation considered here [*Booker*, 1981].

[12] As precise values for the outer scale L_0, the layer thickness D, and the mean square fractional fluctuation of ionisation density $\overline{\left(\frac{\Delta N}{N}\right)^2}$ are not available, a different method for assessing the mean square fluctuation of phase is required.

[13] If, indeed, N_T is the total electron content of the layer considered, with mean square electron content fluctuation $\overline{(\Delta N_T)^2}$, corresponding to fluctuations in
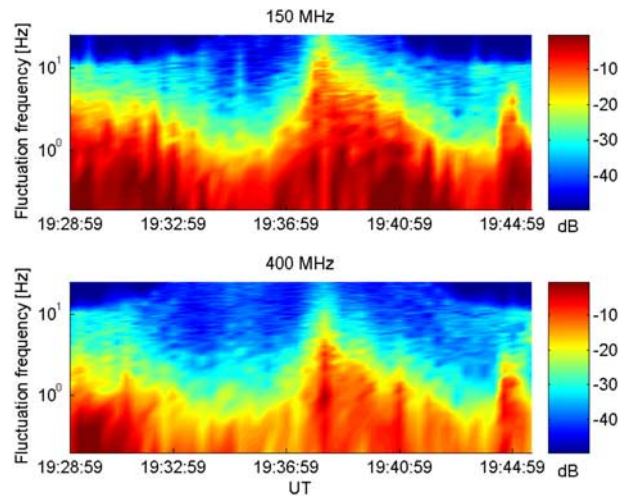

Figure 4. Overview of the intensity spectra observed at 150 MHz and 400 MHz at the ground station located in Kokkola during the night of 30 October 2003, for a satellite pass starting at 19:28:59 UT.
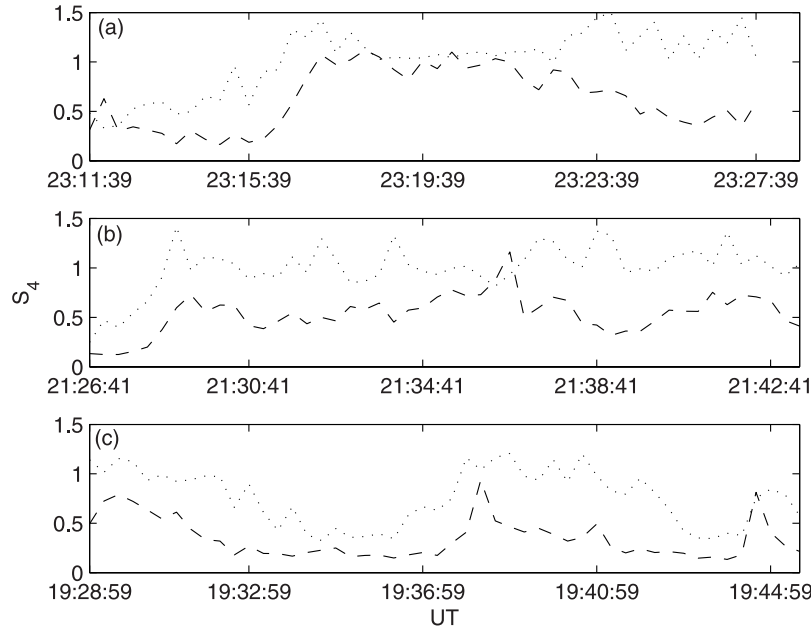
Figure 5. Scintillation indices measured at (a) Kiruna, (b) Lulea, and (c) Kokkola during the satellite passes shown in Figures 2, 3, and 4: 150 MHz (dotted line) and 400 MHz (dashed line).

the ionisation density spatial distribution, the phase fluctuation is

$$\overline{(\Delta\phi)^2} = \lambda^2 r_e^2 B_{\Delta N_T}(0) = \lambda^2 r_e^2 \overline{(\Delta N_T)^2} \qquad (8)$$

where $B_{\Delta N_T}$ is the autocorrelation function for the total electron content fluctuations [*Yeh and Liu*, 1982]. Equation (8) allows for the estimate of $\overline{(\Delta\phi)^2}$ from $\overline{(\Delta N_T)^2}$, actually measured by means of dual frequency phase recording along each slant ray path. The estimate of total electron content fluctuations is carried out over a spectral window consistent with the measured scintillation indices and appropriate to the link geometry.

[14] The Fresnel scale is given by

$$F = \left(\frac{\lambda h \sec \chi}{2\pi}\right)^{1/2} \qquad (9)$$

where λ is the radiation wavelength, h is the height of the phase screen approximating the F region, and χ is the source zenith angle. A value of 300 km is assumed for h, while the values for χ are retrieved from actual satellite positions during the passes considered.

[15] The outer scale L_0 is assumed to be $10F$, while the inner scale L_i is assumed to be $10^{-2}F$, on the order of a few metres and of the ionic gyroradius (i.e., 5 m). Theoretical spectra for intensity fluctuations corresponding to the geophysical conditions occurring during the Tsykhada

measurements have thus been calculated by following as much as possible the theory developed and outlined by *Booker and MajidiAhi* [1981]. The values assumed for the inner scale L_i and particularly for the outer scale L_0 are solely limited to the calculation of the theoretical spectra relative to the case studies considered here.

4. Discussion

[16] Figure 6 shows intensity spectra observed during a satellite pass at the station located in Kokkola. The spectra refer to the 150 MHz signal: the solid line corresponds to a moderate scintillation event ($S_4 = 0.63$), while the dashed line corresponds to a high scintillation event ($S_4 = 1.04$) where saturation is occurring. Figure 7 depicts the theoretical spectra corresponding to the same events in Figure 6: solid line for the moderate scintillation event and dashed line for the high scintillation event. The theoretical spectra are plotted against the spatial frequencies rather than the fluctuation frequencies, as the estimate of the ionospheric relative drift is not attempted here. In the moderate scintillation case, corresponding to a moderate level of the mean square fluctuation of the ionisation density, the calculated spectrum predicts a main lobe and a first side lobe due to Fresnel oscillations. For the remaining lobes, only the average value is shown, indicating a power law behaviour on average which is in agreement with the corresponding observed spectrum (solid line in Figure 6). The difference in the numerical
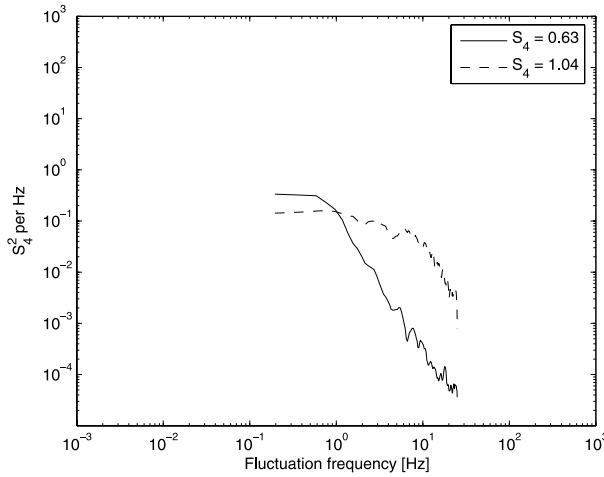
Figure 6. Experimental intensity spectra observed at Kokkola during the night of 30 October 2003 at 19:37:02 UT (full line) and at 19:38:02 (dashed line) for the 150 MHz signal.

values between observed and calculated spectra are due to a not perfect matching between experimental parameter settings and some constant values involved in the theoretical calculations. Nevertheless, as these examples are intended to be purely demonstrative, the main feature to be pointed out is the shape of the power spectral densities rather than their absolute values. It may be noticed,
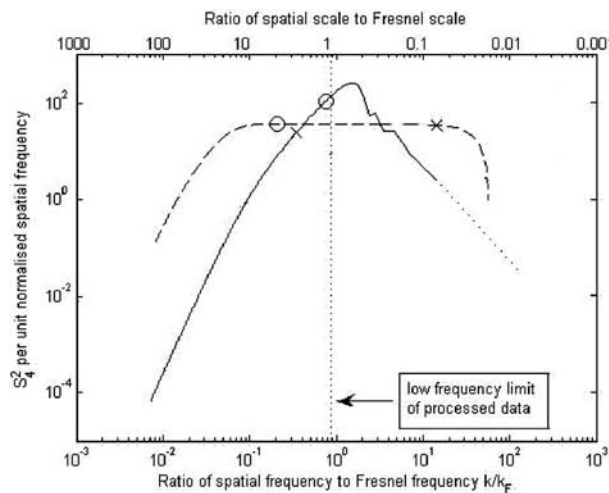

Figure 7. Theoretical intensity spectra calculated on the basis of the refractive theory for the observed spectra shown in Figure 6. Also, the lens scale ('o') and the focal scale ('x') are shown. The vertical dotted line represents the low frequency limit of the detrended experimental data.

indeed, a lowering and a spreading of the calculated intensity spectrum towards both high and low spatial frequencies in the high scintillation case. At high spatial frequencies the roll-off of the intensity spectrum is gaussian and this is a typical situation when refractive scattering dominates over diffractive scattering. The gaussian roll-off shows the existence of a fine structure created in the reception plane by refractive scattering [*Booker and MajidiAhi*, 1981].

[17] The dotted vertical line in Figure 7 shows the low frequency limit of the experimental data detrending process, which reduces the spectral window for the measured data. Only the spectral window pertaining to spatial frequencies higher then the low frequency limit may actually be compared with experimental spectra in Figure 6.

[18] An additional example is provided in Figures 8 and 9, which show observed and calculated intensity spectra, respectively, for the 400 MHz signal recorded at the station located in Lulea, during a moderate scintillation event ($S_4 = 0.45$, solid line) and a high scintillation event ($S_4 = 1.16$, dashed line). During the moderate scintillation event the calculated spectrum predicts a main lobe and a first side lobe with an average power law at high spatial frequencies, which is consistent with the observed intensity spectrum behaviour. On the contrary, in presence of large ionisation density fluctuations, the calculated intensity spectrum predicts a spread towards both low and high spatial frequencies, consistent with the observed spectrum, indicating that refractive scattering from large scale structures is dominating over diffractive scattering and leading to saturation.
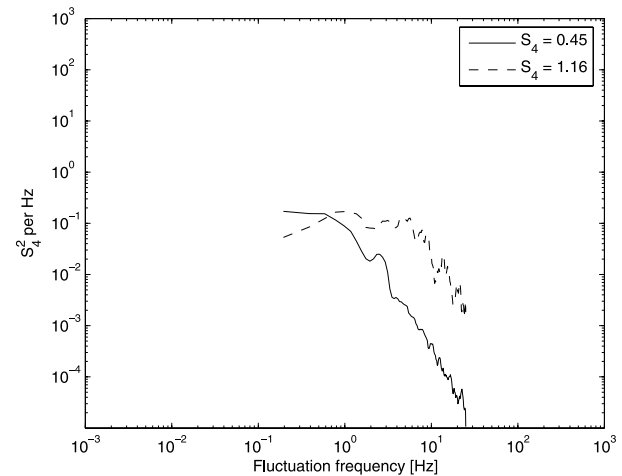

Figure 8. Experimental intensity spectra observed at Lulea during the night of 30 October 2003 at 21:33:44 UT (full line) and at 21:36:41 (dashed line) for the 400 MHz signal.
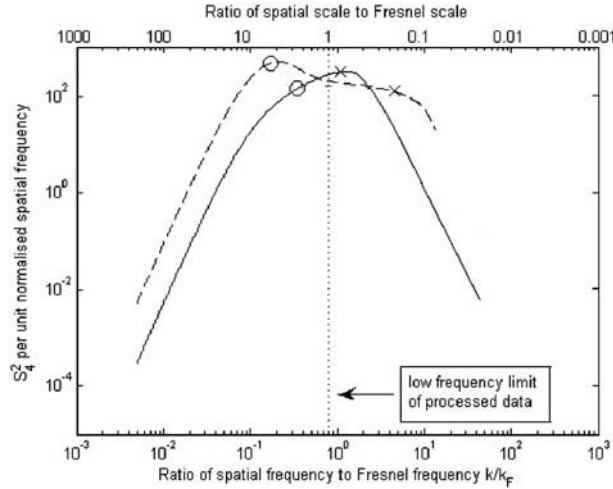
Figure 9. Theoretical intensity spectra calculated on the basis of the refractive theory for the observed spectra shown in Figure 8. Also, the lens scale ('o') and the focal scale ('x') are shown. The vertical dotted line represents the low frequency limit of the detrended experimental data.

[19] Figures 7 and 9 also show the values of lens ('o'), Fresnel, and focal scales ('x') for all the cases considered. In the case of a spectral index of 2 (as for calculated spectra in Figure 7), the lens scale is defined as [*Booker and MajidiAhi*, 1981]

$$L = F\left[2\overline{(\Delta\phi)^2}\right]^{1/4} \qquad (10)$$

while the focal scale is given by

$$l = \frac{L_0}{2\overline{(\Delta\phi)^2}} \qquad (11)$$

[20] As it may be noticed in Figure 7, the conditions corresponding to the moderate scintillation case (solid line) are such that $l > L$ and $l > F$, making lens and focal behaviour negligible. The power spectrum created in the reception plane is that of a typical weak scattering. In this case, indeed, the weak scattering conditions are well expected for a scintillation index $S_4 = 0.63$ at 150 MHz and for a spectral index $p = 2$, as focal and lens scales have not yet crossed each other, leaving diffractive scattering to dominate over refractive scattering [*Booker and MajidiAhi*, 1981]. Again, this is consitent with the behaviour observed in the experimental intensity spectrum for the same moderate scintillation case in Figure 6.

[21] It should be noticed here that no particular spectral features are expected to appear on both theoretical

and experimental spectra at the focal or lens scale. The point is the relative value of the focal scale l with respect to the lens scale L and the Fresnel scale F. When $l > L$, F the lens and focal scale behaviour is negligible and the power spectrum created on the reception plane is due to diffractive scattering. On the contrary, when $l < L$, F then the focal and lens scales start to matter and the power spectrum on the reception plane is rather due to refractive scattering. The values for l, L, and F are indicated on the theoretical spectra only in order to help the reader in the distinction between diffractive and refractive scattering cases, which lead to different spectral shapes. Eventually, the different spectral shapes need to be observed and compared between experimental and theoretical curves, by noticing the spread towards low and high fluctuation frequencies in the refractive scattering cases.

[22] The dashed line curve in Figure 7 depicts a situation where the scintillation activity has risen to a high level, with $S_4 = 1.04$. In this case $l < L$ and $l \ll F$, so that lens and focal behaviour starts to matter. The intensity power spectrum created in the reception plane spreads towards both low and high spatial frequencies with a gaussian roll-off at high frequencies which is somehow not perfectly visible from the calculated curve in Figure 7 due to limitations in the numerical integration method used. As the lens scale is large with respect to the focal scale, lens and focal behaviour play a dominant role. Moreover, the focal scale is also small compared with the Fresnel scale so that saturation occurs.

[23] A slightly different situation is depicted by the solid line curve in Figure 9, corresponding to a moderate scintillation level at 400 MHz with $S_4 = 0.45$, where focal and lens scales are such that $l < F < L$. In this case, the focal scale is given by

$$l = \frac{L_0}{\left[\overline{(\Delta\phi)^2}\ln\overline{(\Delta\phi)^2}\right]^{1/2}} \qquad (12)$$

owing to a spectral index of 3 [*Booker and MajidiAhi*, 1981]. Lens and focal behaviour just starts to matter as the point at which $l = L$ occurs for a S_4 value slightly less than 0.5. Likely, the two scales have just become equal and tend to further separate due to an increasing scintillation activity (Figure 5). The intensity power spectrum observed in the reception plane is going to spread over a larger interval of spatial frequencies, although its high frequency end is very similar to that pertaining to weak scattering.

[24] The dashed line curve in Figure 9 shows a situation similar to that in Figure 7. Here $l < L$ and $l \ll$ F, indicating that refractive scattering is now completely dominating. In particular, the focal scale is smaller than

the Fresnel scale, so that saturation of the scintillation index occurs ($S_4 = 1.16$ at 400 MHz).

[25] It should be noticed that the high frequency roll-off for the strong scintillation events shown in Figures 6 and 8 is about one order of magnitude larger than the similar events measured at low latitudes by *Vats et al.* [1981]. This is due to a relative ionospheric drift (composed by the satellite ray penetration drift at ionospheric altitudes and by the ionospheric plasma density irregularities drift) which is larger for the Tsykada satellites measurements at auroral latitudes presented here than for the geostationary link considered at low latitudes in *Vats et al.* [1981].

5. On the Weak Scattering Theory

[26] Similar results have been obtained in the past by refining the weak scattering theory through the use of numerical methods for calculating a series expansion of the intensity spectral density function (SDF) based on a 1-D phase SDF [*Rino and Owen*, 1984].

[27] These simulations have been applied not only to a single component power law, but also extended to a two component power law for the phase SDF [*Franke and Liu*, 1983; *Rino and Owen*, 1984]. The assumption of a two component power law phase SDF was based on in-situ measurements made at equatorial latitudes [*Basu et al.*, 1983].

[28] The improved weak scattering description seems to be able to explain features such as the spectral broadening similar to what observed by means of the Tsykada signals mesurements presented here. However, a deeper analysis of the improved weak scattering description is needed in order to better understand the physical mechanisms responsible for the observed intensity scintillation events.

[29] The numerical simulations calculated by *Rino and Owen* [1984] and by *Franke and Liu* [1983] were based on a series expansion of the phase SDF, with the assumption of both single and two component power law. In the case of the single component power law, the weak scattering description predicts a departure from the power law (with the intensity SDF spreading towards higher fluctuation frequencies) faster for the spectral index $p = 3$ than for $p = 2$. Referring to *Rino and Owen* [1984], in the case of a perturbation strength parameter value $C_s = 10^{23}$, the simulated intensity SDF for $p = 3$ is already departing from the power law and broadening towards higher fluctuation frequencies, while for the same C_s value (i.e., 10^{23}) the intensity SDF for $p = 2$ still shows a clear power law behaviour (this can be noticed by comparing their Figures 8 and 9). On the contrary, the refractive scattering description predicts a departure from the power law with spreading towards

higher fluctuation frequencies (with corresponding S_4 saturation) faster for $p = 2$ than for $p = 3$, which can be noticed by comparing Figures 2 and 3 of *Booker and MajidiAhi* [1981].

[30] The refractive scattering description appears to be closer to what observed by means of the scintillation measurements presented here. The experimental intensity SDFs shown in Figure 6 (corresponding to two scintillation events, one weak and one strong) are reproduced in Figure 7 by means of the refractive scatering theory. The correct behaviour for the intensity SDF observed during a strong scintillation event (Figure 6) is reproduced with $p = 2$ and not with $p = 3$. The theoretical SDF with $p = 3$, indeed, still shows a power law behaviour for the $\overline{(\Delta\phi)^2}$ value corresponding to the strong scintillation event shown in Figure 6. It should be noticed again that the $\overline{(\Delta\phi)^2}$ values used here for reproducing the theoretical SDFs are obtained direclty from the dual frequency measurements available from Tsykada satellites.

[31] It seems that a different result would have been obtained by applying the weak scattering description. The same feature has been observed for the strong scintillation case shown in Figures 8 and 9.

[32] In the case of a two component power law, the spectral broadening towards higher fluctuation frequencies and departure from the power law is obtained for C_s values even larger than in the case of single component power law. This seems to be evident by comparing Figures 8, 9, and 15 of *Rino and Owen* [1984]. So, taking again into account the events shown in Figure 6 of this paper, a different value of the mean square fluctuation of phase $\overline{(\Delta\phi)^2}$ would have been needed in order to obtain a non-power law behaviour. Nevertheless, a somehow $\overline{(\Delta\phi)^2}$ value larger than what actually measured would not be a realistic one, of course.

[33] Moreover, the assumption of a two component power law phase SDF considered in *Rino and Owen* [1984] and in *Franke and Liu* [1983] was motivated by experimental in-situ measurements at equatorial latitudes [*Basu et al.*, 1983]. The scintillation measurements presented here deals with auroral latitudes ionospheric electron density irregularities, for which there is no indication of two component power law phase SDF. However, this point still needs a deeper analysis.

[34] The refractive scattering theory, based on a single component power law for the phase SDF, seems to provide numerical results and a physical interpretation more appropriate to what has been measured by means of the Tsykada satellites links.

[35] A further evidence of this is provided in Figure 10, where the geometrical factor G has been calculated for the links corresponding to the events shown in Figures 6 and 8. In the weak scattering description, the geometrical
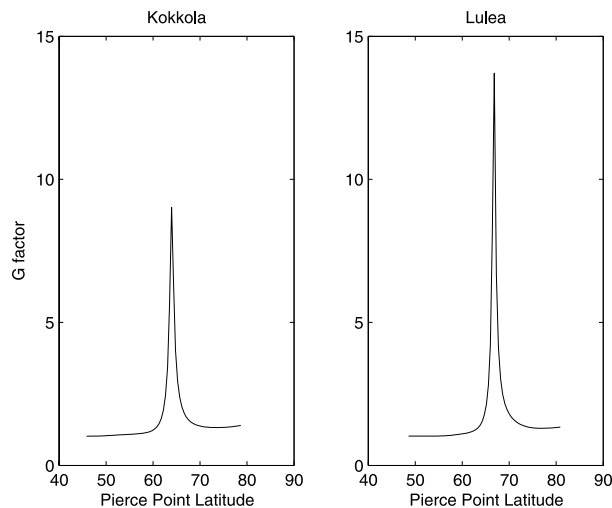
Figure 10. The geometrical factor G calculated for the Tsykada satellite passes osberved at Kokkola (starting at 19:28:59 UT) and at Lulea (starting at 21:26:41 UT).

factor *G* shows narrow localised peaks whenever the ray path lies within an L shell and was introduced in order to explain events with high phase scintillation and low intensity scintillation [*Rino and Matthews*, 1980; *Rino and Owen*, 1980].

[36] By comparing Figures 5 and 10, it is evident that the strong scintillation events (shown in Figures 6 and 8) correspond to high *G* values. Nevertheless, from Figure 5 it is also evident that strong scintillation events are occurring not only in presence of peaks in *G*. The alignment with magnetic field lines proved by the *G* factor suggests only the traversing of large scale structures which should be sheetlike at auroral latitudes and field aligned [*Aarons*, 1982]. This fact is consistent with the refractive scattering caused by large scale electron density irregularities with sizes much larger than the Fresnel scale.

6. Conclusions

[37] Experimental evidence for refractive scattering has been found in radio waves scintillation events after propagation through the disturbed auroral ionosphere during the geomagnetic storm occurred at the end of October 2003. The intensity power spectral densities produced in the reception plane have been found to be spread towards both low and high spatial frequencies, covering a frequency range larger than usual, in presence of high values of the intensity scintillation index S_4.

[38] Overall, high scintillation activity is due to refractive scattering by large scale plasma density irregularities present in the ionosphere along the ray path, while low scintillation activity is rather due to diffractive scattering by plasma density irregularities with scales smaller than the Fresnel scale.

References

Aarons, J. (1982), Global morphology of ionospheric scintillations, *Proc. IEEE*, *70*(4).

Basu, S., S. Basu, J. P. McClure, W. B. Hanson, and H. E. Whitney (1983), High resolution topside in situ data of electron densities and VHF/GHz scintillations in the equatorial region, *J. Geophys. Res.*, *88*(A1), 403–415.

Booker, H. G. (1981), Application of refractive scintillation theory to radio transmission through the ionosphere and the solar wind, and to reflection from a rough ocean, *J. Atmos. Terr. Phys.*, *43*(11), 1215–1233.

Booker, H. G., and G. MajidiAhi (1981), Theory of refractive scattering in scintillation phenomena, *J. Atmos. Terr. Phys.*, *43*(11), 1124–1199.

Briggs, B. H., and I. A. Parkin (1963), On the variation of radio star and satellite scintillations with zenith angle, *J. Atmos. Terr. Phys.*, *25*, 339–365.

Crain, C. M., H. G. Booker, and J. A. Ferguson (1979), Use of refractive scattering to explain SHF scintillations, *Radio Sci.*, *14*(1), 125–134.

Forte, B. (2005), Optimum detrending of raw GPS data for scintillation measurements at auroral latitudes, *J. Atmos. Sol. Terr. Phys.*, *67*, 1100–1109.

Forte, B., and S. M. Radicella (2002), Problems in data treatment for ionospheric scintillation measurements, *Radio Sci.*, *37*(6), 1096, doi:10.1029/2001RS002508.

Foster, J. C., and W. Rideout (2005), Midlatitude TEC enhancements during the October 2003 superstorm, *Geophys. Res. Lett.*, *32*, L12S04, doi:10.1029/2004GL021719.

Franke, S. J., and C. H. Liu (1983), Observations and modeling of multifrequency VHF and GHz scintillations in the equatorial region, *J. Geophys. Res.*, *88*(A9), 7075–7085.

Fremouw, E. J., R. L. Leadabrand, R. C. Livingston, M. D. Cousins, C. L. Rino, B. C. Fair, and R. A. Long (1978), Early results from the DNA Wideband satellite experiment-Complex signal analysis, *Radio Sci.*, *13*(1), 167–187.

Mitchell, C. N., L. Alfonsi, G. De Franceschi, M. Lester, V. Romano, and A. W. Wernik (2005), GPS TEC and scintillation measurements from the polar ionosphere during the October 2003 storm, *Geophys. Res. Lett.*, *32*, L12S03, doi:10.1029/2004GL021644.

Rino, C. L. (1979a), A power law phase screen model for ionospheric scintillation: 1. Weak scatter, *Radio Sci.*, *14*(6), 1135–1145.

Rino, C. L. (1979b), A power law phase screen model for ionospheric scintillation: 2. Strong scatter, *Radio Sci.*, *14*(6), 1147–1155.

Rino, C. L., and S. J. Matthews (1980), On the morphology of auroral zone radio wave scintillation, *J. Geophys. Res.*, *85*, 4139–4151.

Rino, C. L., and J. Owen (1980), The structure of localized nighttime auroral zone scintillation enhancements, *J. Geophys. Res.*, *85*(A6), 1941–1948.

Rino, C. L., and J. Owen (1984), Numerical simulations of intensity scintillation using the power law phase screen model, *Radio Sci.*, *19*(3), 891–908.

Tatarskii, V. I. (1967), *The Effects of the Turbulent Atmosphere on Wave Propagation*, Nauka, Moscow.

Vats, H. O., H. G. Booker, and G. MajidiAhi (1981), Quantitative explanation of strong multifrequency intensity scintillation spectra using refractive scattering, *J. Atmos. Terr. Phys.*, *43*(12), 1235–1241.

Yeh, K. C., and C. H. Liu (1982), Radio wave scintillations in the ionosphere, *Proc. IEEE*, *70*(4), 324–360.

B. Forte, Centre for Atmospheric Research, University of Nova Gorica, Vipavska 13, P.O. Box 301, SI-5001 Nova Gorica, Slovenia. (biagio.forte@p-ng.si)